Sedimentary Geology 344 (2016) 34–46

Contents lists available at ScienceDirect

Sedimentary Geology

journal homepage: www.elsevier.com/locate/sedgeo

Seismically induced liquefaction structures in La Magdalena archaeological site, the 4th century AD Roman Complutum (Madrid, Spain)

M.A. Rodríguez-Pascua [a], P.G. Silva [b], M.A. Perucha [a], J.L. Giner-Robles [c], C. Heras [d], A.B. Bastida [d], P. Carrasco [e], E. Roquero [f], J. Lario [g], T. Bardaji [h], R. Pérez-López [a], J. Elez [b]

[a] Instituto Geológico y Minero de España, Madrid, Spain
[b] Dpto. Geología, Escuela Politécnica Superior de Ávila, Universidad Salamanca, Ávila, Spain
[c] Facultad de Ciencias, Universidad Autónoma de Madrid, Madrid, Spain
[d] Trébede, Patrimonio Cultural, S.L. Torres de la Alameda, Madrid, Spain
[e] Dpto. Ingeniería del Terreno, Escuela Politécnica Superior de Ávila, Universidad Salamanca, Ávila, Spain
[f] Dpto. Edafología, E.T.S.I. Agrónomos, Universidad Politécnica de Madrid, Madrid, Spain
[g] Facultad de Ciencias, UNED, Madrid, Spain
[h] U.D. Geología. Fac. Ciencias, Universidad de Alcalá de Henares, Madrid, Spain

ARTICLE INFO

Article history:
Received 29 October 2015
Received in revised form 21 January 2016
Accepted 29 January 2016
Available online 6 February 2016

Keywords:
Complutum
Earthquake
Liquefaction
Earthquake Archaeological Effects (EAEs)
4th century AD

ABSTRACT

The ancient Roman city of Complutum (Alcalá de Henares, Madrid), founded in the 1st century AD, was one of the most important cities of Hispania. The old Roman city was destroyed, abruptly abandoned, relocated close by and rebuilt during the late 4th century AD. Destruction of the city and its relocation has not yet been explained by archaeologists. In this paper, with our multidisciplinary approach, we identify and characterize earthquake archaeological effects (EAEs) affecting the archaeological site, the La Magdalena, an agricultural holding 4 km from the core of Complutum. The most important EAEs in the site are liquefactions (sand dikes and explosive sand-gravel craters) affecting Roman structures, such as water tanks (cisterns), houses and graves. Ground liquefaction generated significant ground cracks, explosive craters and folds in foundations of buildings. Several other Roman sites throughout the valley were also abandoned abruptly during the 4th century AD, in some cases with EAEs of similar origin. This suggests the occurrence of a 5.0–6.6 Mw seismic event in the zone, in accordance with the minimum empirical limit of seismically-induced liquefaction and the maximum surface rupture length of the Henares fault.

1. Introduction

The archaeological site "La Magdalena", site of the old Roman City of "*Complutum*" (II-IV Century AD), is located in the Henares Valley adjacent to Alcala de Henares (Madrid, Central Spain; Fig. 1). In this site remains have been found: of six occupation phases from the Chalcolithic period (Campanian pottery; c. BC 2500); of two Roman industrial stages, from the Early Imperial period (1st BC – 2nd centuries AD); and of its transformation into a necropolis during the Late Imperial period (3rd to 5th centuries AD). The site also records several later, post-Roman periods of occupation, from 6th to 8th centuries (Visigoth graveyards). During the middle 4th century AD an earthquake shook the site, leaving such evidence as notable ground disruptions, sand ejections, gravel injections and metre-size open craters and ground cracks, affecting Roman industrial buildings and tombs (Rodríguez-Pascua et al., 2015a). Clear anomalies in the Late Roman archaeological record also point to seismic shaking as the main factor influencing the abandoning of the Roman industrial site. In addition to the main city of Complutum, several other sites throughout the valley, most also displaying apparent earthquake archaeological effects (EAEs; Rodríguez-Pascua et al., 2015a), were abruptly abandoned or relocated during the same period. This paper is focused on analysis of the large set of soft-sediment deformation structures (SSDS) found in the archaeological site, as well as on their probable seismic origin. Sand-blown craters affecting pebbles, sand dikes and collapsed terrain, associated with oriented building damage, were also systematically described and mapped. Moreover earthquake environmental effects (EEE) such as ground cracks, mass movement and lateral spreading of river banks were recognized, in agreement with liquefaction features. In light of the foregoing, as the potential seismic source for this historical earthquake we propose an earthquake greater than M5-5.5, and most

E-mail addresses: ma.rodriguez@igme.es (M.A. Rodríguez-Pascua), pgsilva@usal.es (P.G. Silva), ma.perucha@igme.es (M.A. Perucha), jorge.giner@uam.es (J.L. Giner-Robles), cmheras@trebedecultura.com (C. Heras), abbastida@gmail.com (A.B. Bastida), pcarrasco@usal.es (P. Carrasco), elvira.roquero@upm.es (E. Roquero), javier.lario@ccia.uned.es (J. Lario), teresa.bardaji@uah.es (T. Bardaji), r.perez@igme.es (R. Pérez-López), jelez@usal.es (J. Elez).

http://dx.doi.org/10.1016/j.sedgeo.2016.01.025
0037-0738/

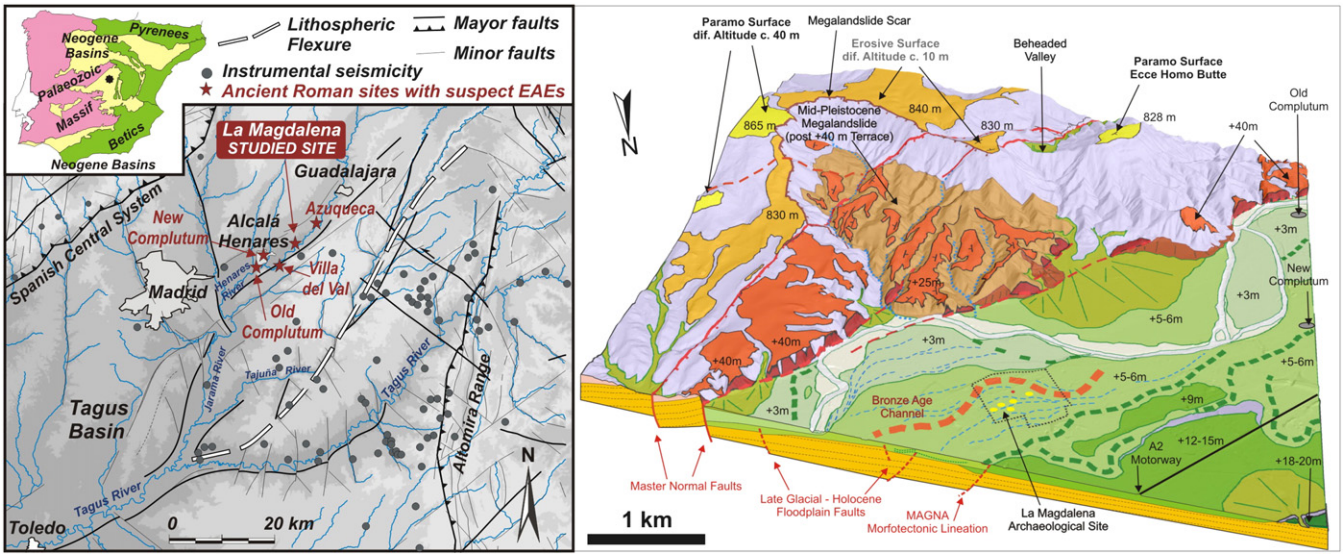

Fig. 1. A) Geographical location and regional geodynamic context of the archaeological Site of La Magdalena, ancient Roman city of Complutum (Alcalá de Henares) and other Late Roman sites in the zone. In the figure are displayed the main recent tectonic features and instrumental seismicity in the whole Neogene Basin. B) Geomorphological sketch of the Henares valley around the studied archaeological site illustrating the most outstanding fluvial and erosive landforms and tectonic features.

probably close to M6, generated by the fault segment of Henares (NE–SW trending) that reached an intensity of ESI 07 on macro-seismic scale IX.

2. Geological and geomorphological setting

The archaeological site of La Magdalena, founded on the Henares River floodplain, +5 m above the present river thalweg, is located in the Tagus Basin (Fig. 1). The site, on the internal edge of a large meander, contains a morpho-sedimentary record of off-lapped sand-gravel point bars and channels, topped by fine-grained (clayey-silts) floodplain deposits (Fig. 2). This fluvial stack (5–10 m thick) of Holocene age is probably older than 4900–4500 years, according to Chalcolithic findings in the archaeological site (Rodríguez-Pascua et al., 2015a). Alluvial sediments overlay thick clayey Miocene materials featured in the sedimentary filling of this area of the Neogene Basin. This implies that

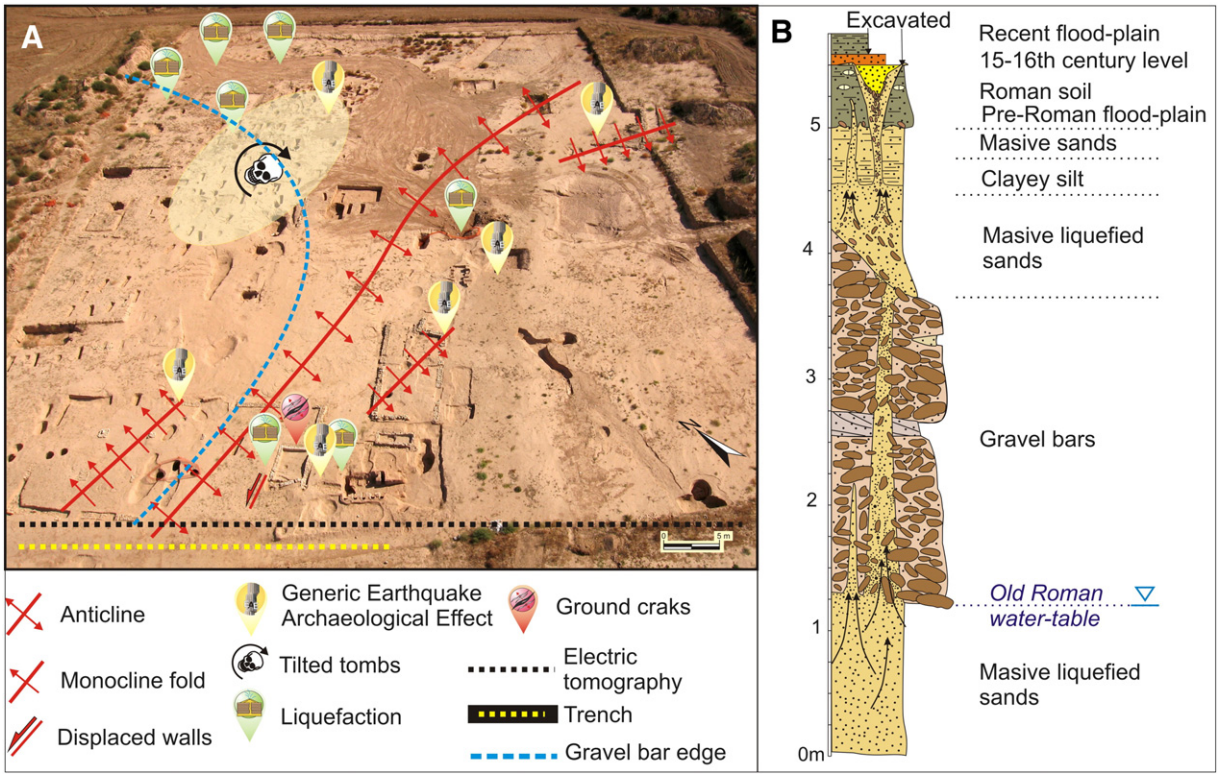

Fig. 2. A) Aerial view of the La Magdalena archaeological site displaying ground surface deformations and recorded EAEs (up), the structure at the bottom of the image corresponds to the Roman tank, surrounded by the labels of the EAEs. B) Simplified stratigraphic-log of the floodplain of the Henares River in the archaeological site of La Magdalena.

the long-term evolution of the area has been dominated by uplift and fluvial down-cutting. This Henares valley zone is characterized by a nearly-linear scarp (40–60 m high) along the southern river margin, probably developed along a NE–SW km-scale normal fault, as proposed by several authors (i.e. Martín Escorza, 1983; Pérez-González and Portero, 2004; Giner et al., 2012). In fact all these authors agree that a large fault zone along the Henares valley affected both the entire Miocene series and the Páramo Surface in the southern valley margin (Fig. 2). Supporting their agreement are both normal faulting recorded in ancient clay quarries around Alcalá (Martín Escorza, 1979) and dislocation of several isolated buttes of the Páramo surface (El Viso, Ecce Homo), 40–50 m below the general elevation of this extensive Late Neogene structural surface south of Alcala de Henares. Several normal faults have also been recorded in the clayey substratum underlying Late Pleistocene terrace deposits downstream from Alcala, on the northern valley margin (+40m from the present Henares River thalweg) (Pérez-González and Portero, 2004). As these authors have observed, the fault zone displaces, by 60–70 m, similar Miocene stratigraphic levels north and south of the valley. More recent studies identify this large fault zone as the northern boundary of a lithospheric-scale flexure, parallel to the Spanish Central System, responsible for instrumental seismicity recorded in the area with magnitudes ≤3.0 mb (Fig. 1; De Vicente et al., 2007; Giner et al., 2012). The last relevant earthquake in the region (1954 San Martin de la Vega earthquake) of magnitude 4.0 mb, was felt with a maximum intensity VI-V MSK in valley zones 10 km from the epicentre (IGN, 1982).

Therefore this event is probably linked with reactivation of the Henares fault zone within the Madrid Basin (Alonso-Zarza et al., 2004; Giner et al., 2012). This fault zone features canyon-like valleys, bounded by relevant kilometric lineal scarps 40–60 m high, related in some cases with moderate historic and instrumental seismicity (Silva, 2003; De Vicente et al., 2007; Giner et al., 2012). Many geomorphologic anomalies and tectonic landforms indicate occurrence of Late Quaternary tectonics in the region (Silva et al., 1988; Giner et al., 1996). Among such geologic evidence indicating tectonic activity are multiple signs of seismically-induced soft-sediment deformations in Middle to Late Pleistocene terrace systems of the Madrid region (Giner, 1996; Giner et al., 1996; Silva et al., 1997; Silva, 2003; Silva et al., 2013). More recent papers provide evidence of complex syn-sedimentary deformations in basal beds of Holocene floodplains along similar fault zones that bound valleys (ie. Jarama fault; Wolf et al., 2013). In all these cases, a thick series of substratum Miocene gypsums has caused some debate on the tectonic origin of these deformations (see discussion in Silva, 2003). However, as mentioned in the introduction, Miocene substratum beneath the archaeological site studied in this paper is composed of thick clayey series (Alonso-Zarza et al., 2004). Historical surface and subsurface soft-sediment deformation structures are reported for the first time in fluvial valleys of the Madrid region in central Spain.

Henares valley has traditionally been considered a "tectonically quiet zone", compared with the numerous deformations and geomorphologic anomalies recorded in Pleistocene fluvial terraces of the

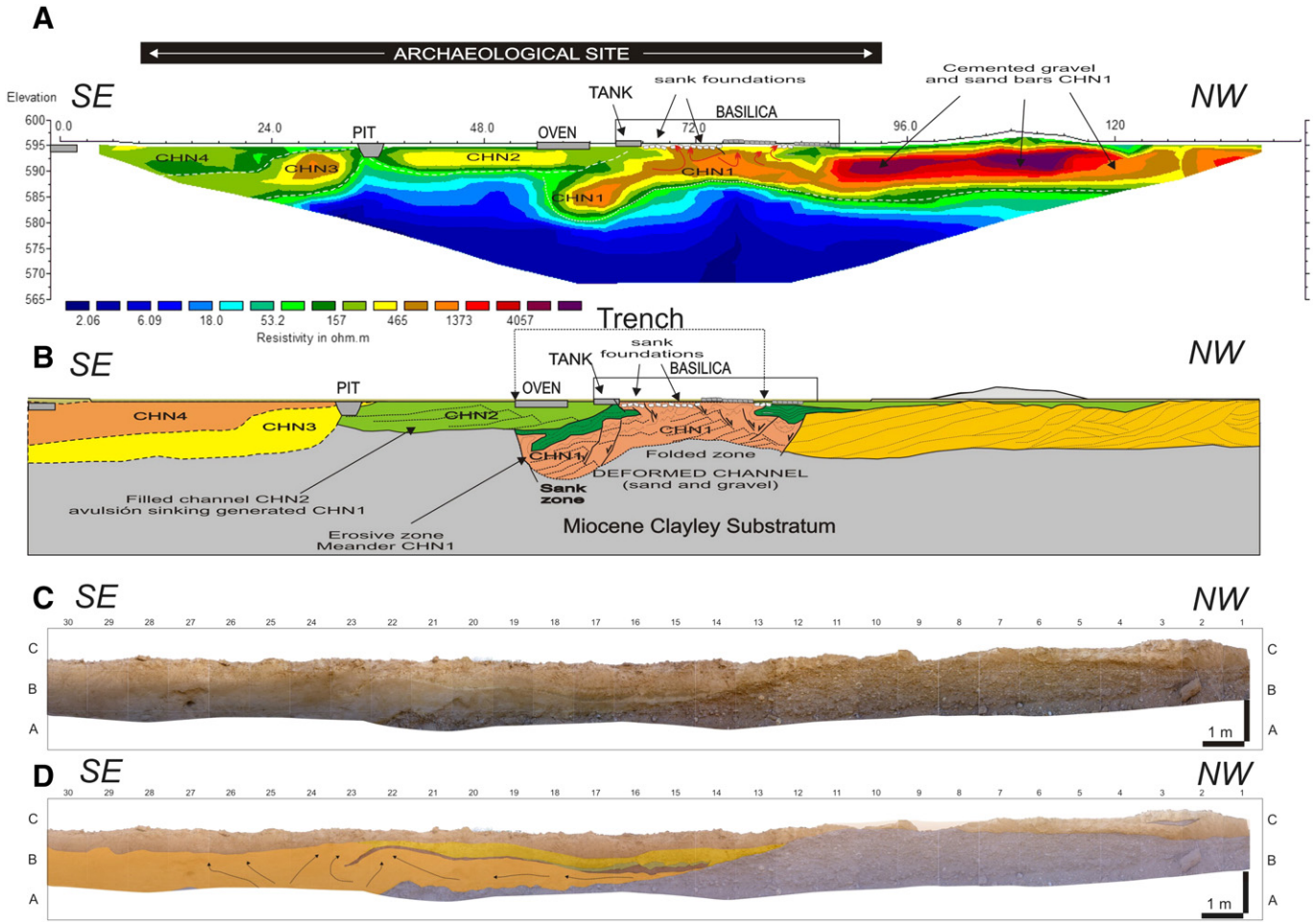

Fig. 3. Paleosismological exploration around of the hydraulic tank (the direction of the sections is N145°E): A) ERT 2D pseudosection displaying deep deformations printed in the point bar—channel sequence underlying the archaeological site; B) Geological interpretational section of the ETR 2D; C) photo mosaic of the trench made parallel to the ERT; D) paleoseismological log of the trench, the arrows show the main direction of flux during the liquefaction.

Table 1
OSL ages of sand samples taken in the exploratory trench (40°30′17.69″N; 3°19′10.15”O). Data from the Luminescence Dating Laboratory of the School of Geography and the Environment (Oxford University; UK). Coloured circles identify the dated samples in the trench logs of Figs. 3 and 4. http://www.geog.ox.ac.uk/research/landscape/old/index.html. Multigrain aliquot measurements and single grain measurements were performed using Risø TL/OSL Mini-sys readers in the coarse grain fraction (180–250 μm) following the standard sample management and dating protocols of the Laboratory.

Sample code	Ground elevation	Burial depth	Depositional environment	Moisture content	Total dose rate Gy/ka	Age (ka BP)
COMP–4 ○	596 m	40 cm	Fluvial: Top flood–plain deposits.	0,01 ± 0,02	No processed	≥ 4.9 – 4.6 (Archaeological dating)
L006/ COMP–3 ○	596 m	110 cm	Fluvial: Upper silty sands (massive)	0,01 ± 0,02	2.94±0.29 (10.04%)	18.53 ± 2.57 (OSL)
L006/ COMP–2 ○	596 m	100 cm	Fluvial: Clean sands (massive) upwarped sand channel	0,01 ± 0,02	1.867± 0,27 (14.65%)	22.85 ± 3.54 (OSL) (15.5%)
COMP–1 ○	596 m	80 cm	Fluvial: Sands in basal gravel bars	0,01 ± 0,02	NO PROCESSED	≥ 18.53 – 22.85 (Relative dating)

Jarama, Tagus and Tajuña valleys (Silva et al., 1988). However, the entire Henares valley displays a regional anomaly, the disparity of the whole set of Plio-Quaternary fluvial terraces on the northern valley slope with the southern slope, characterized by a large linear scarp dissecting the glacis-type surfaces (+40–60 m) from the upper Páramo surface, + 220 m above the current river thalweg (Fig. 1B). Moreover, in the first works on the zone, authors recognized evidence of neotectonic activity and of drastic drainage reorganization along the Henares valley southern margin during the Early-Mid Pleistocene transit, the NE–SW to NW–SE Anchuelo-Pantueña Capture (González Martín and Asensio Amor, 1980), and the NE–SW faults with metric displacements (<5 m) in the clayey Miocene substratum of the southern Henares valley margin (Martín Escorza, 1979). To explain this nearly constant southwards migration of the active river channel throughout the Quaternary, some authors proposed the occurrence of a large fracture zone along the southern Henares River margin (Pérez-González and Portero, 2004). Other authors indicate that marginal large-scale faulting of the active isostatic forebulge within the Madrid Neogene basin has caused the valley's southwards migration (Alonso-Zarza et al., 2004; De Vicente et al., 2007). Whatever the case, given the record of surface and subsurface deformations at the archaeological site studied (Rodríguez-Pascua et al., 2015a), our geological and geomorphological revision of the zone was developed by means of available imagery data, detailed digital elevation models (MDTs) and field survey (Fig. 1B). Our studies indicate the occurrence of a large fracture zone along the southern Henares River margin, vertically displacing the “Páramo surface” about - 40 m. Many fault strands are visible adjacent to the river, some of them featuring well-preserved triangular and trapezoidal facets (Fig. 1B). Additionally, exactly on the opposite margin is a mega-landslide of c. 3.5 km^2 that pulled and dragged the piedmont glacis-type surfaces (+40 m),

Fig. 4. Fractured hydraulic tank I, ground cracks affecting the floor and impact block marks. These fractures are related to liquefaction processes and after this lateral spreading took place. See Fig. 2.

remnants from the "Páramo" surface, dislocated and tilted SW and NW (Fig.1). According to available chronologies for Madrid region valleys (Pérez-González et al., 2013; Silva et al., 2013; Roquero et al., 2015), the mega-landslide would probably have occurred just after development of the +40m terrace, and before or during development of the +18–20 m level. In other words, it should have occurred between c. 400 and 100 ka BP. However, younger but minor reactivations could also have occurred during the relevant base-level fall in the Last Glacial Maximum (Silva et al., 2013).

3. Geophysical prospecting & trenching

In order to identify the nature, thickness and geometry of alluvial deposits beneath the archaeological site, five electric resistivity tomography profiles (ERT), one survey trench, and tens of archaeological digs were made in the studied site. The first ERT profile was made in one of the surface deformations first identified in the site, which induced the fracture and dislocation of a Roman tank, made of 1 m thick hydraulic "*opus caementicium*" in walls and floor (Fig. 2), and several building remains, including an older industrial building with a basilica-like floor plan.

Electric resistivity tomography profiles (ERT Schlumberger array) were made parallel to the southern wall of the basilica building and tank (N150°E; Fig 2). The ERT profile distinguishes a well-developed off-lapped gravel spit-bar system migrating NW-SE. It features highly-resistive quartzite gravel bars (> 1000 Ω/m) preceding development of a set of sand-clayey river channels to the SE (Fig. 3A), characterized by lenticular bodies of the lowest resistivity of the Madrid region (<500 Ω/m). The most significant deformations are in the profile center along the contact of gravel bar deposits and ancient channels, especially in the paleochannel CHN1 (Fig. 3B). This deformed channel is just beneath the basilica building and disrupted tank. In this zone, CHN1 (30 m long × 10 m thick) bends and breaks upwards, while being limited laterally by apparent normal faults inducing abrupt sagging to the SE. It is subsequently replaced by a new un-deformed channel body (CHN2; 20 m long × 6 thick), probably as a consequence of a sudden avulsion process (Fig. 3a and B). An exploratory trench (30 m long × 2.5 m deep) was opened to explore the anomalous deformations distinguished in the ERT profile (Figs. 2 and 3C).

Data from the trench indicate that the deformed fluvial deposits are buried by a regular clayey floodplain level (0.5–0.8 m thick), on which the first archaeological site settlements occur (Chalcolithic silos and graves; BC 2900–2500). This upper level was the former floodplain surface (+5–6 m above the river thalweg) where the deformed buildings described in this work are located. Underlying this upper level, a sandy channel (c. 10 × 1.2 m) bends upwards, anticline-like, exactly under the destroyed tank (Fig. 3D). The channel anticline geometry can be observed in both trench walls, indicating a N100–120°E orientation, congruent with the main directions of ground flexures recorded at the surface (Fig. 2). Surface deformations triggered 10- to 20-cm-amplitude undulations of ancient building foundations, as well as differential subsidence of basilica walls.

Deformation of fluvial sediments was triggered by complete liquefaction of a thick underlying sandy level (c. 1.5–2.8 m thick) in which the sedimentary structures (nicely preserved in adjacent units) were completely blurred by full sand fluidization, extruded

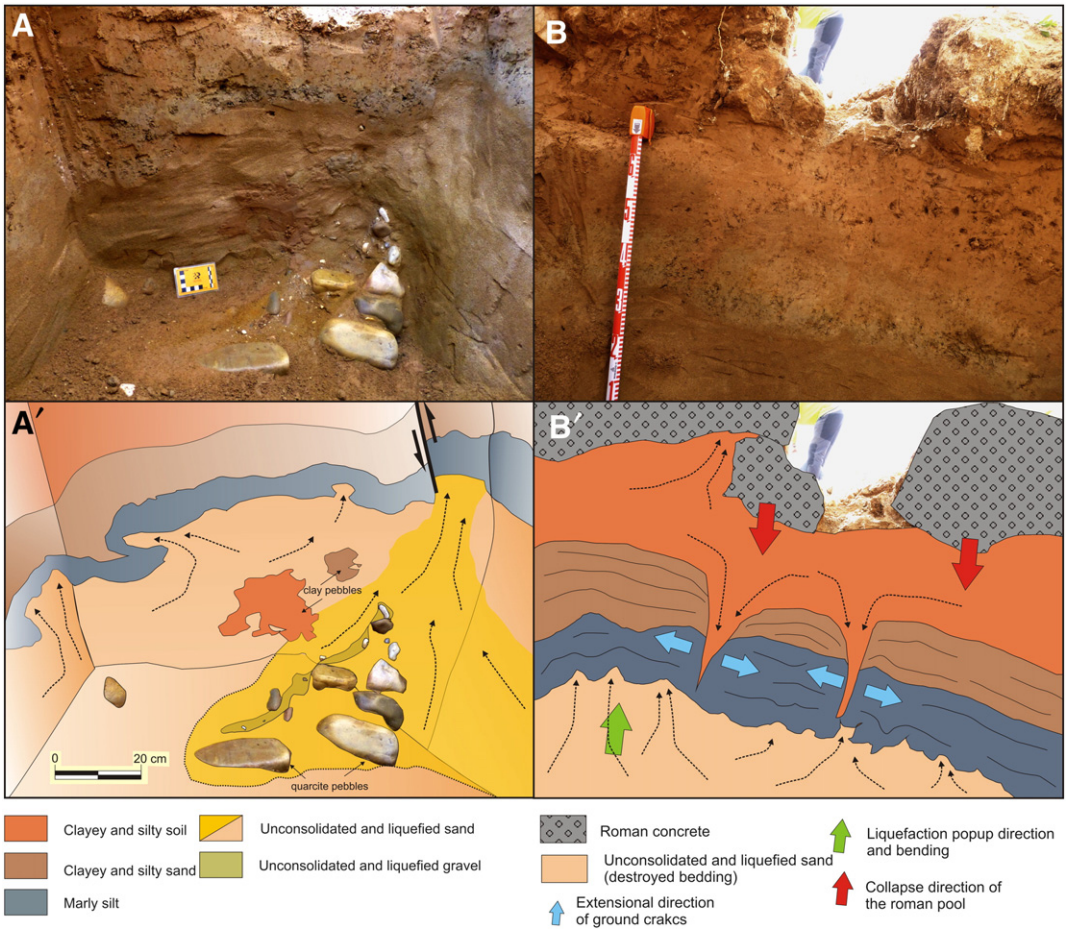

Fig. 5. Photography (A) and interpretational sketch (B) of the liquefaction structures located under the hydraulic tank cistern made of hydraulic mortar. Photography (A) and interpretational sketch (B) of a section in the basement of the hydraulic tank. It is possible observe minor liquefaction structures under the ground cracks.

over the deformed channel (Fig. 3D). The fluidization process also affected sandy gravels outcropping at the trench base, which records apparent injection features. In any case, the large deformations observed in ERT profiles seem to be previous to the Chalcolithic period, but near-surface paleo-liquefaction features recorded in the exploratory trench can be linked to deformations recorded in Roman remains. Therefore, these latter processes seem to be a discrete reactivation of large deformation structures acting in the zone before c. 5,000 yr. BP.

OSL dating carried out in the basal upwarped channel unit and in overlying extruded sands indicates ages of 22,85 ± 3,54 (COMP-2) and 18,53 ± 2,57 (COMP-3) respectively, consistent with basal floodplain deposits in the Tagus basin (Wolf et al., 2013; Silva et al., 2013; Tapias et al., 2012). Consequently, the apparent occurrence of old basal sands in upper floodplain levels strongly supports deeper provenance of the sands, at near-surface locations due both to extrusion linked to paleo-liquefaction features recorded in the exploratory trench and to complex deformation of the old river channel (CHN1), as seen in the ERT profile (Fig. 3). Sample age does not correspond to the age of the liquefaction, but only to the age of sands so affected, presumably coming from 8–10 m depth in the studied site (Table 1).

4. Ground deformations and earthquake archaeological effects

Remains from the Late Imperial Roman period (4th Century AD) excavated at the site show evidence of EAEs in both factory buildings

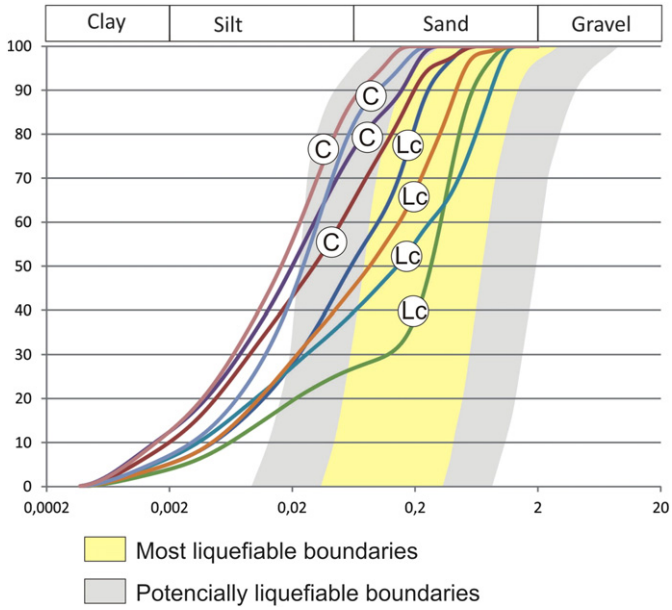

Fig. 7. Granulometric curves of some sediments of the liquefaction strucutres located in the archaeological site. The sampling was performed selecting the confining layer (C) and the intrusion (Lc) separately.

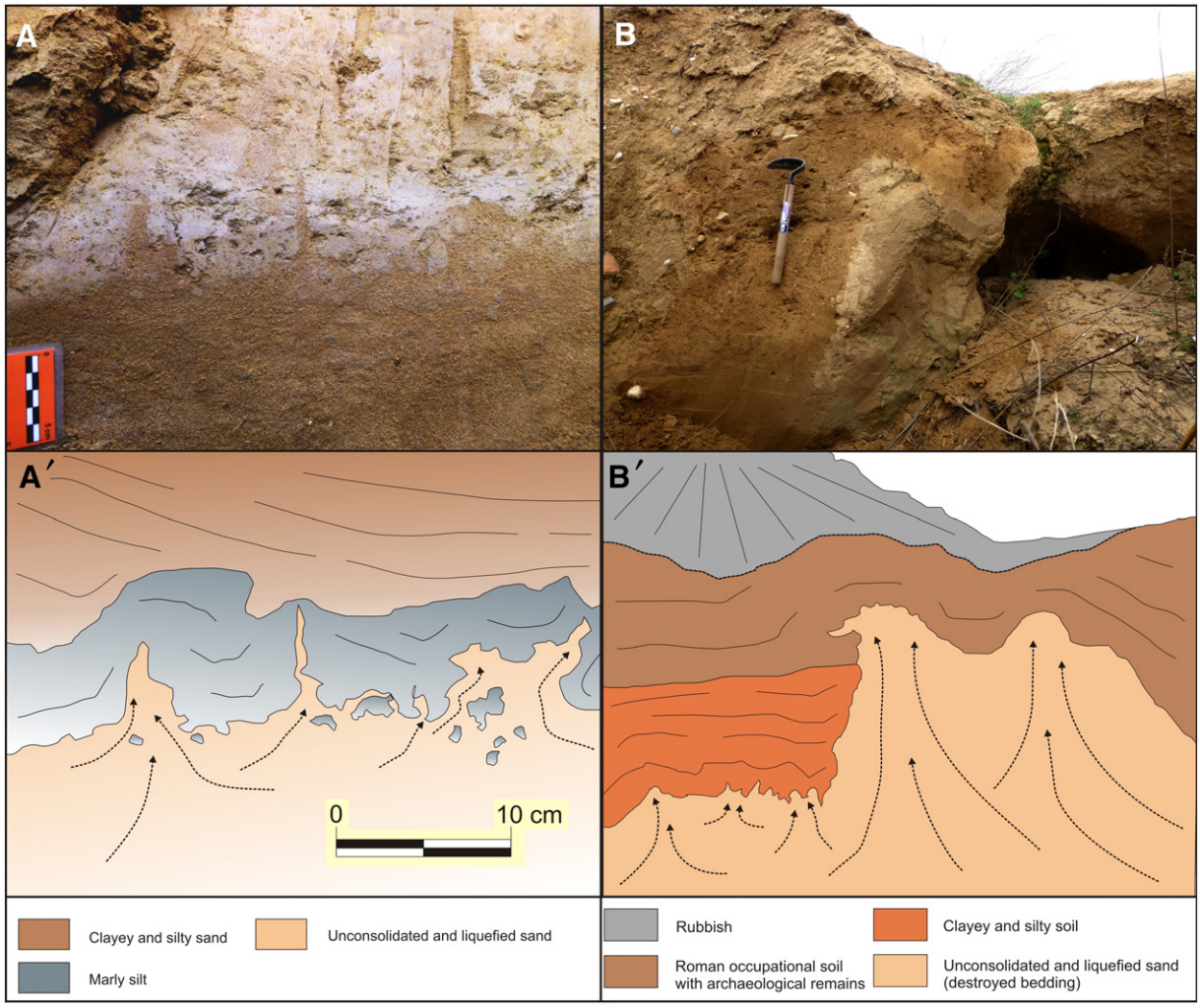

Fig. 6. Photography (A) and interpretational sketch (A´) of the minor liquefaction structures (sand dikes) under the ground cracks. Photography (B) and interpretation (B´) of a sand intrusion affecting the soil with Roman remains. During the excavation, several squared limestone masonry blocs were extracted inside of the liquefied sediments.

and in necropolis remains. All recorded building deformations are closely related to significant paleo-liquefaction features disrupting the ground surface, or preserved in near-surface horizons (<1 m depth). The most significant elements are the following: (a) Open ground cracks and lateral spreading; (b) Near-surface soft-sediment deformations; (c) Sand-gravel explosion craters; (d) Sand-gravel domes; and (e) Burial disruptions. Since most deformations affect Late Roman period remains, all deformations were at first related to strong seismic shaking during the second half of the 4th Century AD (Rodríguez-Pascua et al., 2015a).

4.1. Liquefaction and related open ground cracks

Ground cracks are metric in length with openings up to 30 cm. In one case, ground cracks affect directly a tank built of 1-m thick hydraulic "*opus caementicium*" (Fig. 4), generating fractures and displacements in the archaeological remains. Ground cracks propagated from the foundations, cutting the thick tank floor, clearly continuous with ground cracks preserved in the substratum (presently filled by sands). Consequently, fracturing of such resistant Roman hydraulic concrete can clearly be linked to ground failure, while rejecting building ruin and degradation as causes. The cracked tank floor preserves two significant impact marks superimposed on the cracks, which can be interpreted as the product of local side-wall or roof collapse soon after, or during, abrupt destruction of the tank.

In order to check relationships between ground cracks and fractures affecting the tank, a prospecting trench (1.5 m deep) was opened at the tank base. This water-storage facility is directly founded on a 50 cm thick clayey anthropic level with archaeological remains overlying a 20 cm thick clayey silt level. Underlying sediments are composed of gravelly sands (50 cm) and at least a 40-cm-thick gravel bed of quartzite pebbles embedded in medium-coarse sand (Fig. 5A). Contacts between various units are wavy and irregular, containing cm-scale vertical sand dikes from the lower sandy units intruded in the overlying confining layer of finer sediments (Fig. 5A). The basal gravel bed is intruded in the whole overlying sedimentary sequence, with the apparent vertical mobilization of smaller gravels (3–5 cm) indicating significant liquefaction processes around the destroyed building. In fact, sand dikes were extruded at surface through ground cracks and open fractures in the tank floor, since archaeological excavation encountered the building remains nearly filled by sands.

The liquefaction processes that destroyed the tank triggered differential ground settlement and "lateral spreading", resulting in severe rotation, tilting and collapse of one of the tank sides (Figs. 4 and 5B). In this section small sand dikes can be observed intruding into a marly silt (Fig. 6A). Liquefaction of near-surface (<1 m) sand and gravel levels underlying the site generated observable NE–SW ground folding all over the entire site, affecting different types of structures. Foundations of some buildings (made of rows of fluvial quartzite pebbles) display

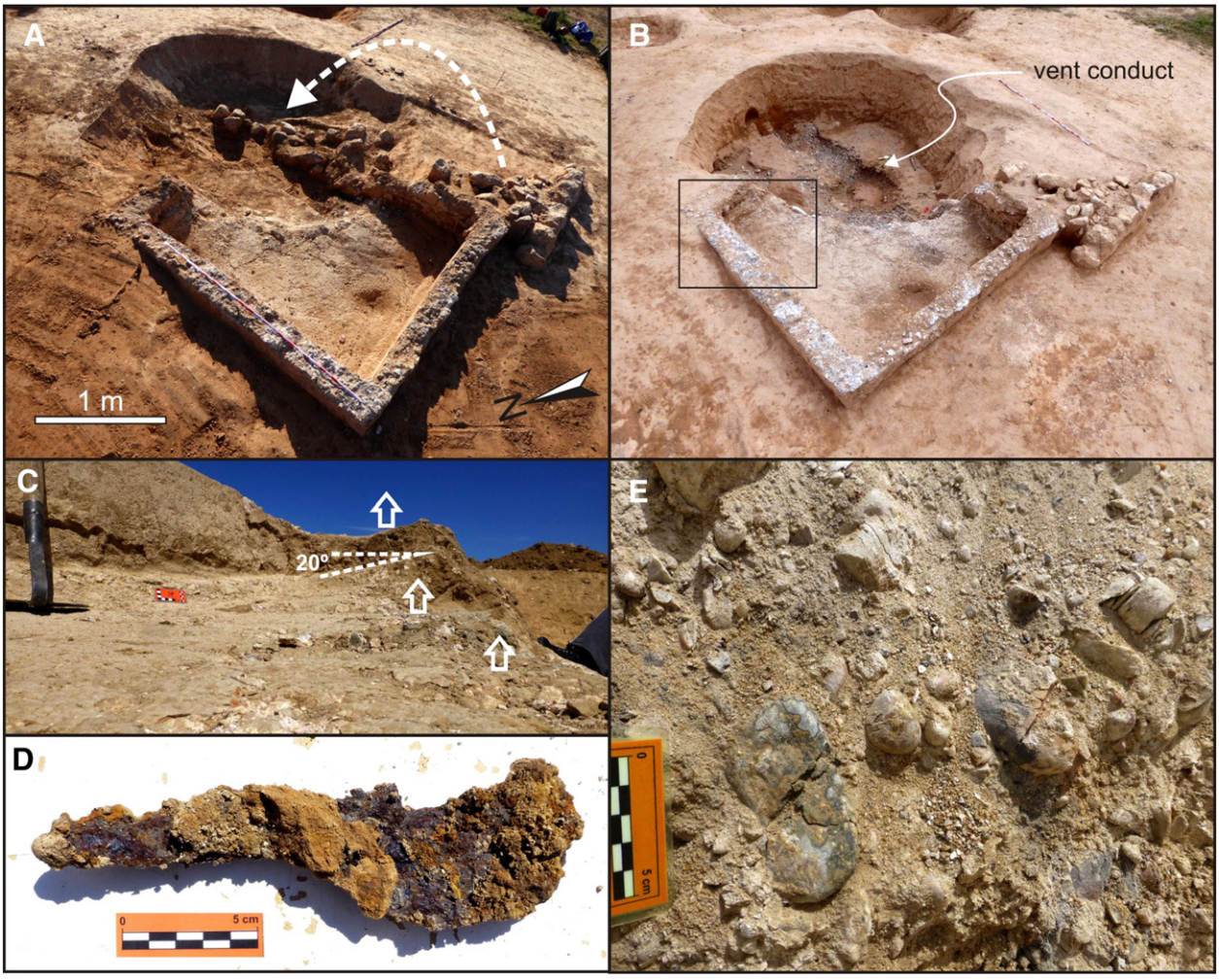

Fig. 8. Sand explosive crater affecting to the hydraulic tank II: A) Initial phase of excavation of the tank II, the white arrow sow the collapse direction of a lateral wall inside of the crater; B) final phase of excavation, the vent conduct is visible in the bottom of the crater; C) lateral close view (square of the Figure B) of the tank basement tilted 20°/323°; D) during the excavation 48 iron Roman tools were extracted from the central part of the crater, one example of a Roman billhook; E) fractured gravels located in the vent conduct, out of the conduct the pebbles are undeformed.

a clear bending, coherent with surface folding. Foundations of the basilica-pattern building, adjacent to the damaged tank, display monoclinal folding and a height difference between its eastern and western zone (c. 50 m apart), on the order of 1 m. Missing SW corner building foundations are taken to be indicative of local sagging, a consequence of surface liquefaction. The unique structure of the site built with heavy masonry blocks (NE sector) thus sank about 3 m below the average archaeological site level (Fig. 6B). Exploratory trenches in one of the sides of the sunken building exposed a N055E vertical sand dike, 1 m wide, sub-parallel to the main folds affecting the site.

Several sand dikes were sampled in order to analyse liquefaction susceptibility of these sediments (Owen and Moretti, 2011). Samples were taken from the intruding sand body and adjacent confining layers (overlaying the liquefied layer). Results of grain size analysis are summarized in Fig. 7. Sands are made up of quartz with carbonate lithics. Grain size ranges from almost pure sands to silt with little clay content (<10%). Sand dikes are composed of 30–60% medium sand. Confining layers are composed mainly of silts (70%). Grain sizes in sand dikes fall within the range of most probably liquefiable sediment limits obtained by Tsuchida and Hayashi (1971), while confining layers are within the lower limit of this range, corresponding to potentially liquefiable boundaries (Fig. 7) (grain size ranging from 0.03 to 0.3 mm). According to this author, these results indicate that the sand dikes could have been generated by an earthquake. Similar results were obtained from grain-size analysis of sands ejected during the Emilia Romagna Earthquakes (May 2012; Mw = 6.1 and 5.9) in Italy (Rodríguez-Pascua et al., 2015b; Fontana et al., 2015).

4.2. Sand-gravel explosion craters

The most representative deformational structures observed in the archaeological site are sand and gravel explosion craters. Circular structures are common in archaeological sites of this epoch, excavated for grain stores or garbage collectors. But several circular structures filled with natural sediments mark the ancient Roman ground surface, and even affect old Roman structures (tanks or cisterns) all around the archaeological site (Figs. 8 and 9).

A crater disrupting a Roman tank, with circular morphology in floor plan view, can be seen in Fig. 8A and B. During the first phase of excavation a thin layer with archaeological remains from the 16th century was encountered. Beneath this upper archaeological layer sands, gravels and a collapsed wall inside the crater were found (Fig. 8A). At this level it is possible to observe that the tank foundations bulged upwards and tilted 20° radially (Fig. 8C). This rounded ground bulge indicates that the sands and gravels rise up from the middle of the circular structure, pushing the ground surface under the tank. In the centre of the crater 48 iron Roman tools, (knives, billhooks, axes, etc.: Fig. 8D) were encountered. Among gravels in the structure centre were several fractured and striated pebbles (Fig. E). A circular structure at the end of the crater is related with the original vent conduit feeding the crater (Fig. 8B).

Seven individual craters were located in the archaeological site (Fig. 9A, B and C). Crater plant-view geometries are clearly circular, like the aforementioned one disrupting the tank. Edges of crater rings are warped upwards (Fig. 9B and C). Upwarping generated circular and radial ground fractures around the crater, visible nowadays in the

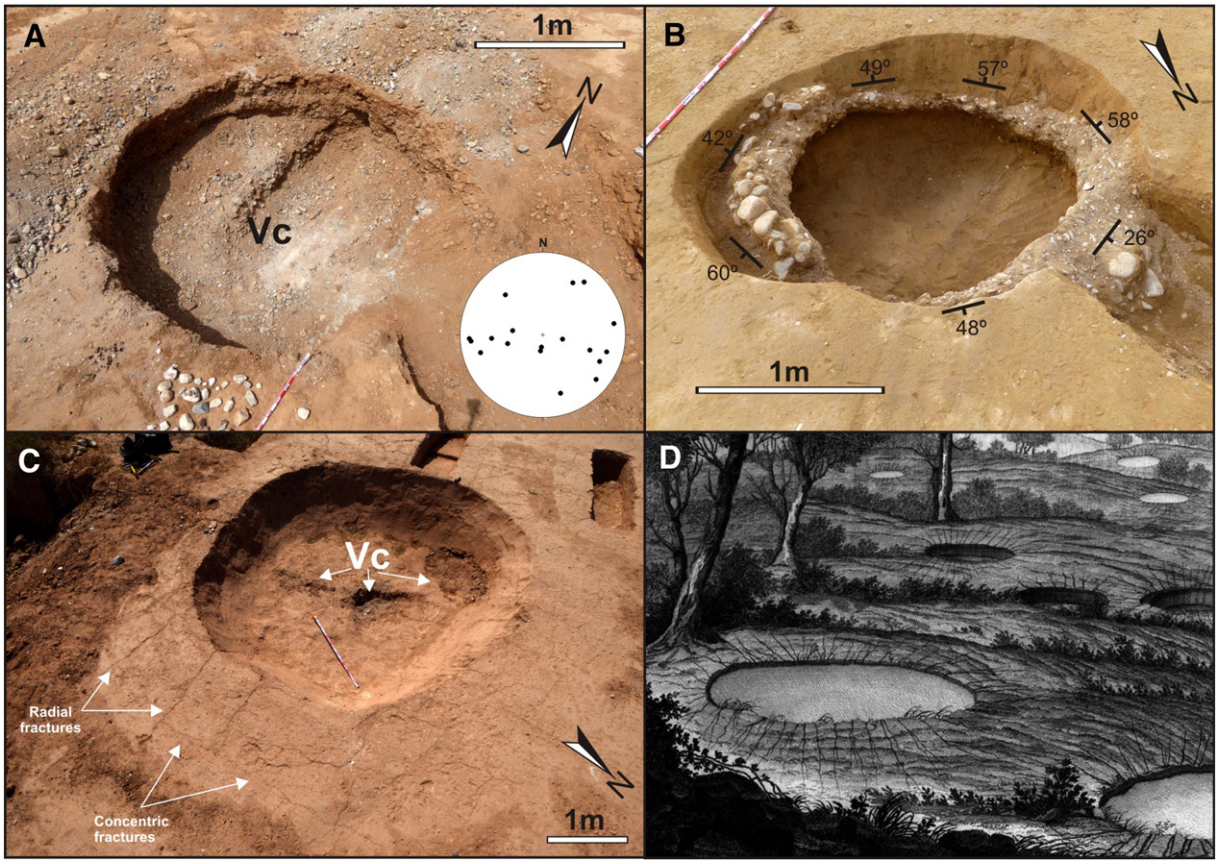

Fig. 9. Explosive sand craters: A) generated in a fluvial gravel bar, in the central part is located the vent conduct (Vc) with fractured pebbles inside, in the stereonet are represented the liquefaction flux directions obtained by the striated pebbles; B) crater affecting to a gravel layer, the morphology is close to a blasted bubble with radial directions; C) crater developed in anthropic carbonaceous silts of Roman age, displaying characteristic radial and concentric fractures. The crater preservers the vent conducts (Vc) which contains sets of fractured and striated pebbles of quartzite; D) Picture of explosive sand craters generated during the 1783 Calabrian earthquake, it is possible observe the radial and circular fractures generated by explosion of liquefied sediments (after Sarconi, 1784).

archaeological site (Fig. 9C). In several cases intrusive sand and gravel sediments were extracted during excavation of the crater. Gravel pebbles display surface striations, showing a dense fracture pattern (Fig. 10). Striated pebble distribution within craters appears as an "outward umbrella" geometry (Fig. 11). Apexes of "outward umbrella gravel" pebbles are nearly smashed, with their matrix composed of a sort of sand and poorly-sorted angular pebble fragments of coarse grain sand (Fig. 10), representing the old vent conduits (Fig. 11). Pebble striations are related with the ductility of the matrix flowing around pebbles during sand extrusion caused by high pore-pressure sediment liquefaction. Using the methodology proposed by Taboada (1993) to determine strain in striated pebbles, flow directions in craters were found to be radial (Fig. 9A), indicating an explosive origin for most craters studied, where pebbles were ejected outwards in all directions around the structure (Fig. 9A y 10). In some cases fractured pebbles expelled from central crater vents also appear in rim deposits around craters (Fig. 11). In one of these craters, illustrated in Fig. 9A, fifty-seven iron Roman tools were encountered during archaeological excavations.

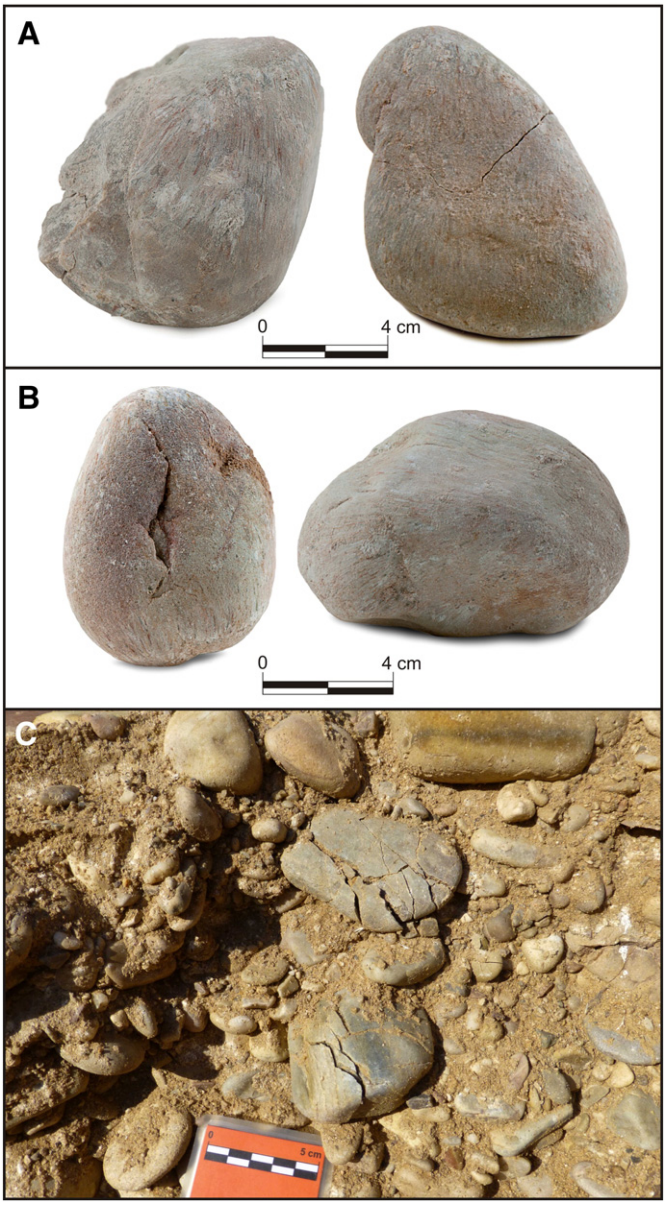

Fig. 10. A: close view of striated pebbles within the sandy matrix located in the vent conduct. It is possible observe the striations, pock marks and fractures. C: Striated and fractured pebbles located in the vent conduct.

Coseismic sand-gravel explosion craters have been documented in several historic earthquakes, such as the AD 1783 Calabria earthquake in southern Italy (IIIX-X MCS; 7.0 Mw; Sarconi, 1784; Fig. 9D). Engravings published by Sarconi (1784) show radial and circular fracture patterns around craters, like those recorded in La Magdalena archaeological site. These fractures were the consequence of explosive extrusion of liquefied sands and interbedded gravel levels, under high pore-pressure conditions. Explosion craters protruded from the ground surface, generating elevated rims and subsequent radial and circular ground cracks, their elevations an indication of the approximate maximum ground up warping. Amick et al. (1990) describe 15–20 cm thick rim deposits around craters generated during the AD 1886 Charleston earthquake (X MM; 7.0 Mw; USA) in response to widespread liquefaction and multiple sand venting in the Mississippi floodplain. These types of ephemeral deposits are poorly preserved in the geological record. Several (c. 10 cm thick) rim deposits were found in the archaeological site studied.

Maximum crater diameter described for the AD 1886 Charleston earthquake was 6 m. La Magdalena crater diameters ranged from 1 to 4.30 m. Infilling of craters from the Charleston Earthquake are a sequence of five layers, composed of vented sand and fragments of the confining layer, sealed by the last phases of soil development after the earthquake (Obermeier, 2009). Common La Magdalena crater infilling is composed of vented sand and fractured pebbles in the vent conduit and an upper layer of gravels with striated and fractured pebbles (with "outward umbrella" geometry) (Fig. 11). The uppermost layer corresponds to unstructured anthropic infilling of sand and Roman pottery (massive) burying an undisturbed archaeological level with pottery remains from the 15th century AD. In two of the craters studied (including one affecting a tank), 105 iron Roman tools were extracted from the upper massive anthropic infilling. Most tools appeared near the vent conduits and over the "outward umbrella" gravel levels, mysteriously, seemingly thrown into the crater after the explosion by the Romans.

Magnitude of an earthquake causing these liquefaction structures is estimated from comparison of liquefaction effects with those observed worldwide and laboratory modelling. The empiric limit for liquefaction of sand sediments is M > 5–5.5 (Atkinson, 1984; Thorson et al., 1986; Scott and Price, 1988; Audemard and De Santis, 1991; Papadopoulos and Lefkopoulos, 1993; Marco and Agnon, 1995; Obermeier, 1996). The main shock of the 1783 Calabria Earthquake, estimated as close to Mw 7.0 (Jacques et al., 2001), generated explosive sand craters. Others examples are craters generated during the 1964 Niigata earthquake of Mw 7.5 (Katayama et al., 1966) or the Charleston earthquake (Ms 7.0; Obermeier, 2009). However, Complutum maximum magnitude is constrained by the maximum rupture length of the Henares Fault, of a surface length of c. 20 km, running along the southern valley margin at a minimum distance from the studied site of about 1 km (Fig.1). The radius of most probable liquefaction is around 25 km from the seismic source (Galli and Ferreli, 1995; Galli, 2000; Rodríguez et al., 2006). Consequently, this fault can be considered to be the most probable seismic source, with the study zone located in the epicentre area (c. 1 km away) of a ≥ 5.0 Mw event. As we shall see, this magnitude range also matches commonly used empirical magnitude relationships with surface rupture length (i.e. Wells and Coppersmith, 1994).

4.3. Anomalies in the Necropolis (Forensic EAEs)

The main area of the necropolis in the northern part of the site is altered (Fig. 4) and contains several burial phases. The early phase belongs to the early imperial period (≤3rd century AD) while the second one belongs to the 4th century AD. In many of the graves in this last burial level, where the deceased were buried in wooden coffins, wood remains and iron coffin spikes were found, along with, in most cases, skeletons tilted and disturbed (pelvis displaced towards thorax, crania

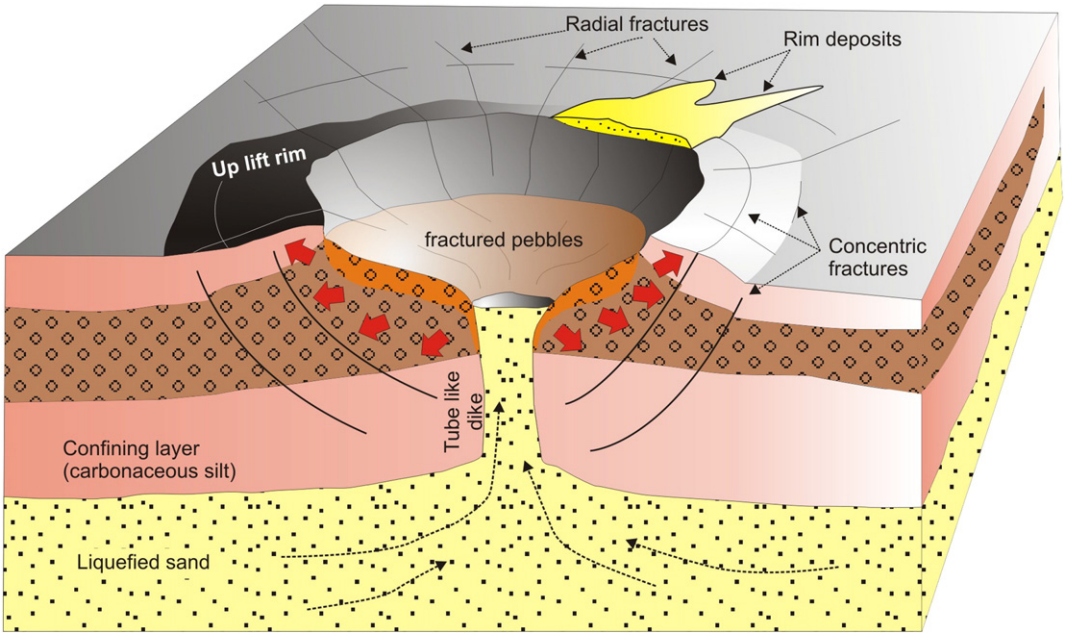

Fig. 11. Idealistic model and section of a sand explosive crater, like that showed in Fig. 9C.

displaced from neck, or a mixture of jumbled bones: Fig. 12). This particular burial level would seem to have undergone ground shaking and liquefaction, stirring and tumbling skeletons (after loss of bone cohesion) within coffins. It is noteworthy that earlier Roman burials (without coffins), as well as subsequent burials (Visigoth graves) in the zone did not undergo such post-mortem disturbance. Cases have been documented of severe burial disturbance due to seismically-induced landslides and liquefaction in historical earthquakes in Spain, from intensity levels ≥ VIII MSK (i.e. 1884 AD Arenas del Rey event), that triggered ejection of coffins (Pérez-López and Rodríguez-Pascua, 2015). This particular *post-mortem* forensic EAE will be the subject of further detailed analyses of bone-displacement vectors to reconstruct dominant ground movement direction.

5. Discussion and conclusions

Deformation structures in La Magdalena archaeological site can be categorized according to the EAE classification of Rodríguez-Pascua et al. (2011), which considers the two outstanding geological coseismic effects of: (1) Sand ejections and sand-gravel explosive craters affecting buildings and necropolis; (2) Open ground cracks and folded substratum. Both are caused by ground liquefaction and differential settling,

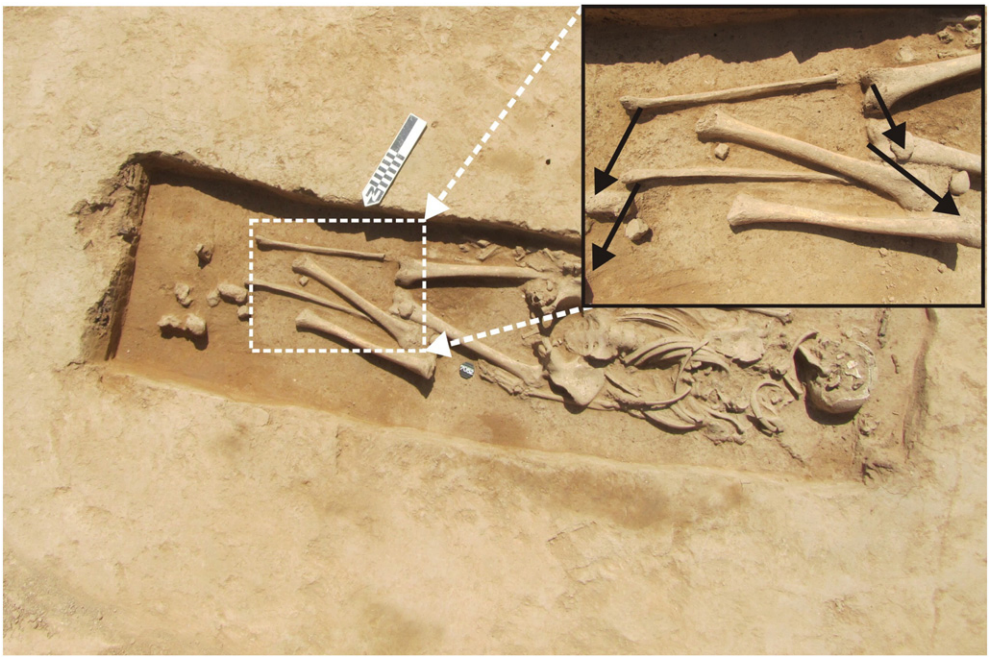

Fig. 12. One example of disturbed tomb located in the archaeological site of La Magdalena. The bone of the legs and feet are displaced northward. These phenomena took place when the skeleton could move inside the coffin.

EEEs considered on the ESI-07 scale (Michetti et al., 2007) from intensity levels ≥VIII, according to observed dimensions. Archaeological remains record three noticeable primary coseismic effects in the building fabric: (1) Tilted and folded walls throughout the entire site; (2) Broken and displaced walls (tank); and (3) Impact block marks (tank). To these common archaeological effects the necropolis adds a new type of forensic EAE, i.e. disturbed skeletons in 4th century AD burials. The most representative liquefaction structure in La Magdalena archaeological site is the sand-gravel explosion crater, structures that affected Roman facilities. Romans would seem to have interacted with the structures by throwing in iron tools, possibly to appease the wrath of the gods (earth and fire). Another crater characteristic is the striation and fracturing of pebbles, caused by hydraulic pressure during the liquefaction and fluidization phenomena.

During the 4th Century, industrial buildings on the site were abandoned. The zone was used only as a graveyard during late Roman and Visigoth times (≤8th Century AD). Although there are no clear signs of abrupt abandon at the site studied, many other Roman settlements around the area record sudden abandoning, or related anomalies during the 4th century AD (Fig. 1; Gómez-Pantoja, 2013). Fires and subsequent abandoning, inexplicable changes in building patterns and land-use are recorded in the houses of "*Hippolytus*" and "*Los Grifos*", in *Complutum* 7 km SE of the site (Rascón Marqués, 2007); "*Villa de El Val*" rural settlement in the Henares Valley about 4 km away (Rascón Marqués et al., 1991); and Azuqueca de Henares 8 km NE (Cardín and Cuadrado, 2013). Additionally, the zone records the abrupt abandonment of the main city of *Complutum*, soon after (c. AD 350) its period of Monumental development (AD 275–300). The city was abandoned and re-located about 2 km away in its present-day location (Alcalá de Henares, Gómez-Pantoja, 2013). An area of at least 50 km^2 along the Henares Valley contains abundant archaeological anomalies dating from the second half of the 4th century AD, closely related to the deformation period identified in La Magdalena archaeological site. Consequently this ancient earthquake should be dated from AD 350 to AD 400, during the second half of the 4th century AD.

Deformations observed can certainly be related to abrupt extensive liquefaction of near-surface sandy levels (c. 5–6 m depth), as shown by geophysical prospecting, exploratory trenching and data from old Roman wells excavated in the zone, these last reaching a maximum depth of 6 m (depth of the old water-table). In addition OSL age data from the exploratory trench (Table 1) clearly indicate that old sand levels (c. 16–19 kyr BP) located in the floodplain base (c. 8–10 m depth) were injected in more surficial levels (2–1.5 m depth) by extensive liquefaction. Data from ERT profiles from the archaeological site show complex deformation of floodplain, channels and old sandy gravel bars, maybe related to previous paleoseismic events occurred before the first Chalcolithic settlements in the site (c. 5.000–5.500 yr. BP). Late Roman liquefaction triggered formation of outstanding sand explosion craters, ground cracking, sand ejections and differential ground settlement. This set of processes damaged Roman buildings while permanently marking the ancient ground surface with deformations. In addition, ground shaking disrupted skeletons in the burial level corresponding to the second half of the 4th century AD.

Such extensive liquefaction in sand-grain-size material would require at least a 5.0–5.5 Mw earthquake, according to empirical studies of seismically-induced liquefaction in the near-field (i.e. Obermeier, 1996). Considering commonly used empirical relationships between magnitude and surface rupture length (i.e. Wells and Coppersmith, 1994), the maximum magnitude related to the adjacent Henares Fault (c. 20 km long) turns out to be 6.6 Mw. For this reason we calculate

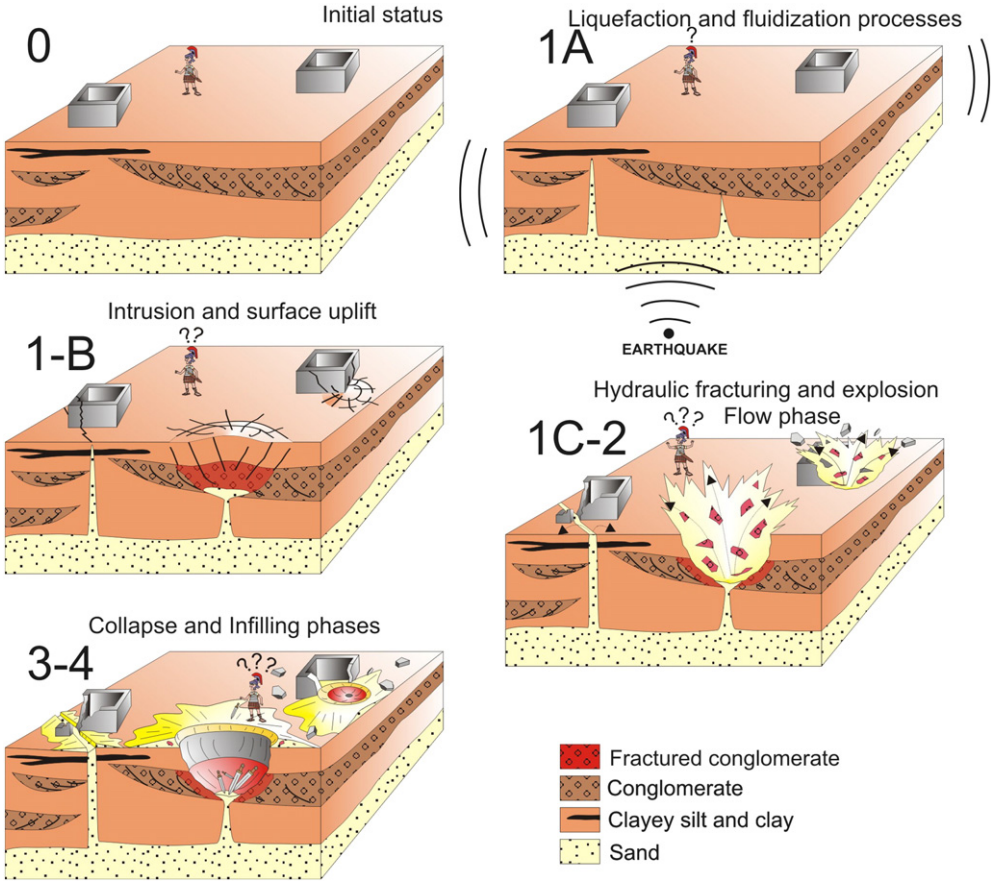

Fig. 13. Evolutionary genetic sketch of sand explosive craters and sand dikes in the archaeological site of La Magdalena.

that the magnitude triggering the extensive liquefaction structures in La Magdalena archaeological site ranged from 5.0 to 6.6 Mw. On the other hand, consideration of the dimension and frequency of sand craters (> 3 m) and ground cracks (> 0.5 m) recorded throughout the site (c. 10.000 m^2) leads to a local seismic intensity of at least IX ESI-07 (Michetti et al., 2007). Obviously, seismic shaking amplification (site effect) was conditioned by thick, (c. 10 m) recent, poorly consolidated fluvial sediments, a shallow water-table (5–6 m), nearly saturated liquefiable sandy levels at depth (6–10 m) and a top clayey confining layer composed of c.0.7–1.1 m thick floodplain deposits. This confining layer was crucial to formation of sand explosion craters.

Evolutionary phases of a single sand explosion crater, as described by Gohn et al. (1984) are: 1—Explosive phase; 2—Flow phase; 3—Collapse phase; 4—Infilling phase. Evidence from the site studied supports a more detailed scheme for the first phase (explosive), divided in these three steps (Fig. 13): 1A—Underground liquefaction and fluidization of sediments beneath the confining layer; 1B—Increasing pore-pressure triggering sediment intrusions and surface upwarping (bulging); 1C—Strong pore-pressure under upwarped confining layer triggering its hydraulic fracture along with abrupt sand and gravel ejection, to generate sand explosion craters. Phase 1A constitutes classical liquefaction of a potentially liquefiable layer, overlapped by a confining, or partially confining, layer as in the case of craters described by Amick et al. (1990) and Amick and Gelinas (1991). Phase 1B is characterized by intrusion of liquefied sand in overlaying sediments. When this liquefied layer penetrates a permeable layer, such as gravels, sand can intrude laterally, with quickly increasing water pore-pressure. Liquefied sand flowing among pebbles generated striations in pebble surfaces and bulging of the ancient ground surface. Phase 1C is characterized by the sharp rise of hydraulic pressure, triggering fracturing and crushing of even very resistant quartzite pebbles, and eventual explosions when shear strength of the confining layer is exceeded. After the explosions, open craters were used by Romans as garbage dumps. In some craters Romans dumped a significant amount of iron hardware (spikes, points, knifes, etc.: Figs. 8 and 13), probably after having witnessed the extensive liquefaction, crater explosions, the subsequent flow phases and destruction of buildings and industrial facilities. One hypothesis is that these iron tools were thrown into open craters as offerings to the gods, to appease the violence of the elements of nature. After this the site was abandoned and other inhabitants used craters as rubbish dumps during the 15th century, as the uppermost centimetre-scale infilling shows. Lower infilling sediments came from the fluvial floodplain of the Henares River.

This ancient earthquake exceeded the intensity and maximum magnitude levels of instrumental and historical records for central Spain. In fact this densely populated zone (2,800 inhabitants/km^2), close to the Madrid urban area (30 km away), is at present outside the area of application of the Spanish Seismic Building Code, which assumes maximum PGA values lower than 0.049 g (IGN, 2013). However, assuming PGA-intensity interval values listed by the IGN (2013) for seismic events of intensity (EMS98) ranging between VIII and IX, a PGA interval ranging between c. 0.19 and 0.39 g could be considered for this event. The empirical relationship between earthquake intensity and PGA value are described for the Iberian Peninsula in the IGN (2013) publication on improvement of the Seismic Hazard Map of the Iberian Peninsula. This value was obtained from the combination of relationships proposed by Atkinson and Kaka (2007) and Faenza and Michelini (2010), and for a recurrence interval of 475 years (IGN, 2013, p. 150). Therefore the unearthing of such "lost earthquakes" in these populated areas is critical for updating seismic hazard assessments in Central Spain.

Acknowledgements

This work is a contribution of the Spanish projects CATESI-07 (IGME-MINECO), CGL2012-37281-C02.01 (QTECTBETICA-USAL), CGL2013-47412-C2-2-P (SISMOSIMA-IGME).

References

Alonso-Zarza, A.M., Calvo, J.P., Silva, P.G., Torres, T., 2004. La Cuenca del Tajo. In: Vera, J.A. (Ed.), Geología de EspañaSociedad Geológica de España. SGE-IGME, Madrid, pp. 556–561.
Amick, D., Gelinas, R., 1991. The search for evidence of large prehistoric earthquakes along the Atlantic coast. Science 251, 655–658.
Amick, D., Gelinas, R., Maurat, R., Cannon, D., Moore, D., Billington, E., Kemppinen, H., 1990. Paleoliquefaction features along the Atlantic seaboard. *NUREG/CR-5613 RA. U.S. Nuclear Regulatory Commision*. Washington DC.
Atkinson, G., 1984. Simple computation of liquefaction probability for seismic hazard applications. Earthquake Spectra 1 (1), 107–123.
Atkinson, G.M., Kaka, S.I., 2007. Relationships between felt intensity and instrumental ground motion in the Central United States and California. Bulletin of the Seismological Society of America 97, 497–510.
Audemard, A., De Santis, F., 1991. Survey of liquefaction structures induced by recent moderate earthquakes. Bulletin of the International Association of Engineering Geology 44, 5–16.
Cardín, I., Cuadrado, M.A., 2013. Yacimiento del Polígono UG XVI de Azuqueca de Henares. In: Cerdeño, M.L., Gamo, E., Sagardoy, T. (Eds.), *La romanización en Guadalajara, arqueología e historia*. La Ergástula, Madrid (España), pp. 137–144.
De Vicente, G., Vegas, R., Muñoz-Martín, A., Silva, P.G., Andriessen, P., Cloetingh, S., González-Casado, J.M., Van Wees, J.D., Álvarez, J., Carbó, A., Olaiz, A., 2007. Cenozoic thick-skinned and topography evolution of the Spanish Central System. Global and Planetary Change 58, 335–381.
Faenza, L., Michelini, A., 2010. Regression analysis of MCS intensity and ground motion parameters in Italy and its implications in shake-map. Geophysical Journal International 180, 1138–1152.
Fontana, D., Lugli, S., Marchetti Dori, S., Caputo, R., Stefani, M., 2015. Sedimentology and composition of sands injected during the seismic crisis of May 2012 (Emilia, Italy): clues for source layer identification and liquefaction regime. Sedimentary Geology 325, 158–167.
Galli, P., 2000. New empirical relationships between magnitude and distance for liquefaction. Tectonophysics 324 (3), 169–187.
Galli, P., Ferreli, L., 1995. A methodological approach for historical liquefaction research. Association of Engineering Geologists Special Publication 6, 35–48.
Giner, J.L., 1996. Análisis neotectónico Y sisnotectónico en El sector Centro-Oriental de La Cuenca Del Tajo PhD. Thesis Universidad Complutense de Madrid, Madrid (325 pp.).
Giner, J.L., de Vicente, G., Pérez González, A.C., Sánchez Cabañero, J.G., Pinilla, L., 1996. Crisis tectónicas cuaternarias en la Cuenca de Madrid. Geogaceta 20 (4), 842–845.
Giner, J.L., Perez-Lopez, R., Silva, P.G., Jiménez Díaz, A., Rodriguez-Pascua, M.A., 2012. Recent tectonic model for the Upper Tagus Basin (Central Spain). Journal of Iberian Geology 38, 113–126.
Gohn, G.S., Weems, R.E., Obermeier, S.F., Gelinas, R.L., 1984. Field studies of earthquake-induced, liquefaction-flowage features in the Charleston, South Carolina, area preliminary report. U.S. Geological Survey Open-File Report 84-67 (35 pp.).
Gómez-Pantoja, J., 2013. Complutum y su territorio. In: Cerdeño, M.L., Gamo, E., Sagardoy, T. (Eds.), *La romanización en Guadalajara, arqueología e historia*. Ed. La Ergástula, Madrid (España), pp. 63–72.
González Martín, J.A., Asensio Amor, I., 1980. Evolución Geomorfológica de los valles del Anchuelo y Pantueña, al sur de Alcalá de Henares (Madrid). Revista de Materiales y Procesos Geológicos 7, 125–145.
IGN, 1982. Catálogo de Isosistas de La Península Ibérica. Instituto Geográfico Nacional. Publicación 202. IGN, Madrid (324 pp.).
IGN, 2013. Actualización de Mapas de Peligrosidad Sísmica en España 2012. Instituto Geográfico Nacional, Madrid (267 pp.).
Jacques, E., Monaco, C., Tapponnier, P., Tortorici, L., Winter, T., 2001. Faulting and earthquake triggering during the 1783 Calabria seismic sequence. Geophysical Journal International 147 (3), 499–516.
Katayama, S., Fujii, T., Takahashi, Y., 1966. Damage caused by the Niigata earthquake and the geological features of National Highway in the suburbs of Niigata City. Soils and Foundations 6, 54–70 (Jpn. Soc. Soil Mech Found. Eng.).
Marco, S., Agnon, A., 1995. Prehistoric earthquake deformations near Masada, Dead Sea graben. Geology 23, 695–698.
Martín Escorza, C., 1979. Fallas y fracturas en las capas miocenas de Alcalá de Henares (Madrid): Interpretación tectónica. Estudios Geológicos 35, 599–604.
Martín Escorza, C., 1983. La neotectónica de la Cuenca de Madrid. *Geología de España (Libro Jubiliar J.M. Rios)* vol. 2. IGME, Madrid (Spain), pp. 543–553.
Michetti, A.M., Esposito, E., Guerrieri, L., Porfido, S., Serva, L., Tatevossian, R., Vittori, E., Audemard, F., Azuma, T., Clague, J., Comerci, V., Gurpinar, A., Mc, Calpin J., Mohammadioun, B., Morner, N.A., Ota, Y., Roghozin, E., 2007. Intensity Scale ESI 2007. In: Guerrieri, L., Vittori, E. (Eds.), Memorie Descrittive Carta Geologica d'Italia., 74, Servizio Geologico d'Italia – Dipartimento Difesa del Suolo, APAT, Roma (53 pp.).
Obermeier, S.F., 1996. Use of liquefaction-induced features for paleoseismic analysis. Engineering Geology 44, 1–76.
Obermeier, S.F., 2009. Using liquefaction-induced and other soft-sediment features for paleoseismic analysis. In: McCalping, J.P. (Ed.), Paleoseismology, second ed. Academic Press, London, pp. 497–564.
Owen, G., Moretti, M., 2011. Identifying triggers for liquefaction-induced soft-sediment deformation in sands. Sedimentary Geology 235, 141–147.
Papadopoulos, G.A., Lefkopoulos, G., 1993. Magnitude-distance relations for liquefactions in soil from earthquakes. Bulletin of the Seismological Society of America 83 (3), 925–938.
Pérez-González, A., Portero, J.M., 2004. Mapa Geológico de España 1.50.000. Alcalá de Henares (560)MAGNA ª Serie. IGME, Madrid (52 pp.).
Pérez-González, A., Gallardo-Millán, J.L., Uribelarrea del Val, D., Panera, J., Rubio-Jara, S., 2013. La inversión Matuyama-Brunhes en la secuencia de terrazas del río Jarama

entre Velilla de San Antonio y Altos de la Mejorada, al SE de Madrid (España). Estudios Geológicos 69 (1), 35–46.
Pérez-López, R., Rodríguez-Pascua, M.A., 2015. Los Terremotos Perdidos (Ed. IGME-Catarata. 118 pp.).
Rascón Marqués, S., 2007. La así llamada casa de Hippolytus: la fundación de los anios y la schola de una agrupación colegial de la ciudad romana de Complutum. Archivo Español de Arqueología 80, 119–152.
Rascón Marqués, S., Méndez Madariaga, A., del Río Español, P.D., 1991. La Reocupación del mosaico del Auriga victorioso en la villa romana del Val (Alcalá de Henares). Un estudio de microespacio. Arqueología, Paleontología y Etnografía 1, 181–200.
Rodríguez, L.M., Audemard, F., Rodríguez, J.A., 2006. Casos históricos de licuación en sedimentos inducidos por sismos en Venezuela desde 1530. Revista de la Facultad de Ingeniería de la U.C.V. 21 (3), 5–32.
Rodríguez-Pascua, M.A., Pérez-López, R., Silva, P.G., Giner-Robles, J.L., Garduño-Monroy, V.H., Reicherter, K., 2011. A comprehensive classification of Earthquake Archaeological Effects (EAE) for archaeoseismology. Quaternary International 242, 20–30.
Rodríguez-Pascua, M.A., Heras, C., Bastida, A.B., Giner-Robles, J.L., Silva, P.G., Perucha, M.A., Roquero, E., Carrasco, P., Pérez-López, R., Lario, J., Bardaji, T., 2015a. New insights on the occurrence of ancient earthquakes in Central Spain: archaeoseismology of the Complutum area (4th century AD, Madrid). Miscellanea INGV 27, 402–405.
Rodríguez-Pascua, M.A., Silva, Pablo G.P.G., Perez-Lopez, R., Giner-Robles, J.L., Martín-Gonzalez, F., Del Moral, B., 2015b. Polygenetic sand volcanoes: on the features of liquefaction processes generated by a single event (2012 Emilia Romagna 5.9 Mw earthquake Italy). Quaternary International 357, 329–335.
Roquero, E., Silva, P.G., Goy, J.L., Zazo, C., Massana, J., 2015. Soil evolution indices in fluvial Terrace chronosequences from central Spain (Tagus and Duero fluvial basins). Quaternary International 376, 101–113.
Sarconi, M., 1784. Historia de Fenomeni del Tremuoto Avvenuto Nella Calabria e Nel Valdemone nell'anno: Posti in Luce Alla Reale. Acc. Delle Scienze e delle Belle Lettere di Napoli, Napoli (70 pp.).
Scott, B., Price, S., 1988. Earthquake-induced structures in young sediments. Tectonophysics 147, 165–170.
Silva, P.G., 2003. El Cuaternario del Valle inferior del Manzanares. Estudios Geológicos 59, 107–131.
Silva, P.G., Goy, J.L., Zazo, C., 1988. Neotectónica del sector centromeridional de la Cuenca de Madrid. Estudios Geológicos 44, 415–427.
Silva, P.G., Cañaveras, J.C., Sánchez-Moral, S., Lario, J., Sanz, E., 1997. 3D soft-sediment deformation structures: evidence for quaternary seismicity in the Madrid basin, Spain. Terra Nova 9, 208–212.
Silva, P.G., López Recio, M., Tapias, F., Roquero, E., Morín, J., Rus, I., Carrasco, P., Rodríguez Pascua, M.A., Pérez-López, R., 2013. Stratigraphy of the Arriaga Palaeolithic sites. Implications for the geomorphological evolution recorded by thickened fluvial sequences within the Manzanares River valley (Madrid Neogene Basin, Central Spain). Geomorphology 196, 138–161.
Taboada, T., 1993. Stress and strain from striated pebbles. Theoretical analysis of striations on a rigid spherical body linked to a symmetrical tensor. Journal of Structural Geology 15, 1315–1330.
Tapias, F., Lóopez Recio, M., Manzano, I., Alcaraz, M., Morín, J., Sese, C., Dapena, L., Alarcon, A., Yravedra, J., Arteaga, C., 2012. Geoarqueología y paleontología de los depósitos del Pleistoceno Superior del antiguo Arroyo Abroñigal (Cuenca del Manzanares, Madrid): el yacimiento del Puente de los Tres Ojos. Cuaternario y Geomorfología 26 (1–2), 105–132.
Thorson, R.M., Claiton, W.S., Seever, L., 1986. Geologic evidence for a large prehistorical earthquake in eastern of Connecticut. Geology 14, 463–467.
Tsuchida, H., Hayashi, S., 1971. Estimation of liquefaction potential of sandy soils. Proc. Third Joint Meeting, US–Japan Panel on Wind and Seismic Effects, UJNR, Tokyo, May, pp. 91–109 (1971).
Wells, D.L., Coppersmith, K.J., 1994. Empirical relationships among magnitude, rupture length, rupture area, and surface displacement. Bulletin of the Seismological Society of America 84, 974–1002.
Wolf, D., Seim, A., Díaz del Olmo, F., Faust, D., 2013. Late Quaternary fluvial dynamics of the Jarama River in central Spain. Quaternary International 302, 20–41.